

## The decomposition of supersaturated $\text{Al}_{1-x}\text{Si}_x$ solid solutions

This article has been downloaded from IOPscience. Please scroll down to see the full text article.

1994 J. Phys.: Condens. Matter 6 9079

(<http://iopscience.iop.org/0953-8984/6/43/013>)

View [the table of contents for this issue](#), or go to the [journal homepage](#) for more

Download details:

IP Address: 171.66.16.151

The article was downloaded on 12/05/2010 at 20:54

Please note that [terms and conditions apply](#).

## The decomposition of supersaturated $\text{Al}_{1-x}\text{Si}_x$ solid solutions

N E Sluchanko†, V V Glushkov†, S V Demishev†, A K Savchenko‡ and V V Brazhkin§

† General Physics Institute, Russian Academy of Sciences, Vavilov Street 38, 117942 Moscow, Russia

‡ Department of Physics, University of Exeter, Stocker Road, Exeter EX4 4QL, UK

§ Institute of High-Pressure Physics, Russian Academy of Sciences, 142092 Troitsk, Moscow Region, Russia

Received 7 June 1994, in final form 26 July 1994

**Abstract.** The decomposition kinetics of supersaturated FCC  $\text{Al}_{1-x}\text{Si}_x$  solid solutions has been studied in the wide concentration range  $x \leq 0.1$  by the resistivity relaxation method and the differential scanning microcalorimetry technique. It was established by an original ‘set of steps’ isothermal annealing procedure that the spinodal boundary probably occurs at  $x \simeq 0.08$  in these substances and the last stages of the decomposition process correspond to coagulation with  $\Delta\rho \sim t^{-1/5}$  behaviour at intermediate temperatures.

The kinetics of phase separation after quenching into the miscibility gap has been studied in a variety of two-phase systems ranging from liquid mixtures to solid alloys [1, 2]. The dominant processes observed are the demixing of the homogeneous system into single-phase regions and the consequent increase in the average size of these regions, known as coarsening.

In the late stages of this coarsening process the scaling behaviour has been predicted and measured experimentally using small-angle scattering of neutrons, x-rays or light [1, 2]. One of the prominent examples of decomposition studies was obtained by investigation of the phase separation kinetics of Cu–Fe alloys by small-angle x-ray scattering and Mössbauer spectroscopy [3].

Another of the most convenient objects to study this class of phenomena are non-equilibrium substitutional solid solutions consisting of metal and semiconductor elements such as  $\text{Al}_{1-x}\text{Si}_x$  and  $\text{Al}_{1-x}\text{Ge}_x$ . As opposed to Al–Si and Al–Ge alloys, produced by rapid quenching at ambient pressure [4–6], the substitutional solid solutions  $\text{Al}_{1-x}\text{Si}_x$  and  $\text{Al}_{1-x}\text{Ge}_x$  are homogeneous polycrystalline materials that can be obtained under high-pressure treatment [7, 8]. At the same time the high-pressure treatment technique surely supplies conditions that are favourable to eliminate the formation of quenched in excess vacancies or vacancy aggregates [4–6] during the synthesis procedure. Moreover the peculiarities of the phase  $T$ – $C$  diagram of Al–Si and Al–Ge systems under pressure allow one to reach significant enhancement of the Si and Ge solubility in Al and for  $\text{Al}_{1-x}\text{Si}_x$  the value  $x = 0.2$  has already been achieved [9]. Simultaneously the increase of Si content creates a rise of the superconductive transition temperature up to 11 K among the solid solutions  $\text{Al}_{1-x}\text{Si}_x$  [9] and so the non-equilibrium state of Si in the FCC lattice and enhanced superconductivity are very closely associated with each other in these substances [10].

In this paper we have investigated the details of the decomposition process in FCC supersaturated  $\text{Al}_{1-x}\text{Si}_x$  solid solutions that causes Si precipitate formation in the Al rich

matrix. The samples of non-equilibrium FCC  $\text{Al}_{1-x}\text{Si}_x$  solid solutions ( $x < 0.12$ ) have been obtained by high-pressure (up to 10 GPa) treatment in the Toroid chamber [11].

As it is known from [12] the decomposition process occurs in a temperature range 360–560 K in  $\text{Al}_{1-x}\text{Si}_x$  but until now there was no information on the kinetics of the phase transition or any experimental results on the precise isothermal phase transition curves in these solid solutions. It appears very important to investigate the ‘set of steps’ in the decomposition process such as rapid relaxation during the first stage and the coagulation and coalescence during the later ones. Another interesting problem is to find the boundary of spinodal decomposition for  $\text{Al}_{1-x}\text{Si}_x$  as predicted by Binder [13].

To study the isothermal phase transformation curves in  $\text{Al}_{1-x}\text{Si}_x$  we investigated time dependences of the resistivity  $\rho(t)$  at different temperatures  $T_{\text{an}}$ . The resistivity against temperature curves  $\rho(T)$  were studied to find the residual resistivity value variation during the Si content changes. Additional information was obtained from x-ray analyses and FCC lattice parameter determination. DSC curves were also recorded to connect the resistivity changes with the heat release during the transformation. The sample preparation and selection procedure has been described elsewhere [10].

One of the similarly obtained resistivity relaxation curves is presented in figure 1. It corresponds to Si concentration  $x = 0.075$  and one can find on it two different sections at least. The first process is rapid and causes the most significant part of  $\Delta\rho(t)$  changes in  $\text{Al}_{1-x}\text{Si}_x$ . The second looks like rather slow relaxation to the equilibrium resistivity value. As was established from DSC experiments the first process is connected with noticeable heat release (figure 2). Calorimetric curves demonstrate a single-peak structure in the concentration range  $x < 0.08$  and only small traces of additional anomaly  $\dot{H}(T)$  are present but then with increasing Si concentration an additional heat release peak appears (figure 2). The activation energies were determined from both of these peaks by a standard procedure during isochronal annealing with various heating rates. The calculated values are  $E_{a1} = 95 + 15 \text{ kJ mol}^{-1}$  and  $E_{a2} = 120 + 15 \text{ kJ mol}^{-1}$  respectively and are closely related to the results [12] where average activation energy  $E_a = 110 \text{ kJ mol}^{-1}$  was obtained in Al–Si alloys.

It is very important to establish the features of the substitution process in  $\text{Al}_{1-x}\text{Si}_x$ . For this purpose we have measured the residual resistivity variation during the Al to Si substitution. The family of resistivity temperature dependences was recorded in the wide temperature range 2–300 K (figure 3). From the data of figure 3 one can notice that for solid solutions  $\text{Al}_{1-x}\text{Si}_x$  with Si content  $x > 1.5$  at.% the residual resistivity  $\rho_0$  exceeds the value  $5 \times 10^{-7} \Omega \text{ cm}$  and the low-temperature contribution of the impurity scattering mechanism becomes dominant. The residual resistivity changes  $\rho_0(x)$  in solid solutions  $\text{Al}_{1-x}\text{Si}_x$  (the inset in figure 3) are essentially non-monotonic: the value  $\rho_0(x)$  changes noticeably in the composition range 0–3 at.% Si and for  $x > 0.08$ , while for concentrations  $0.03 < x < 0.08$   $\rho_0(x)$  remains constant. To clarify the nature of these peculiarities the measurements were repeated after annealing at  $T_{\text{an}} > 500 \text{ K}$ ,  $t = 20 \text{ min}$  on the Al–Si alloy samples. The difference  $\Delta\rho_0$  (10 K) (figure 3) between the initial and final curves is mainly determined by the value of residual resistivity  $\rho_0(x)$  of the sample in the initial stage. Thus, from the data of the inset in figure 3 one can possibly conclude that non-monotonic residual resistivity changes of solid solutions are due to peculiarities of Al to Si substitution in the FCC lattice of  $\text{Al}_{1-x}\text{Si}_x$ .

At the same time in the case of FCC substitutional solid solutions AB with random atom arrangement according to evaluation [14] one can expect that for  $x_c = 2\text{--}3$  at.% the dimer concentration (dimers are Si pairs surrounded by Al atoms) becomes equal to the monomer one (Si atoms surrounded by Al only) and for  $x \geq x_{c2} = 8\text{--}9$  at.% polyatomic clusters of B

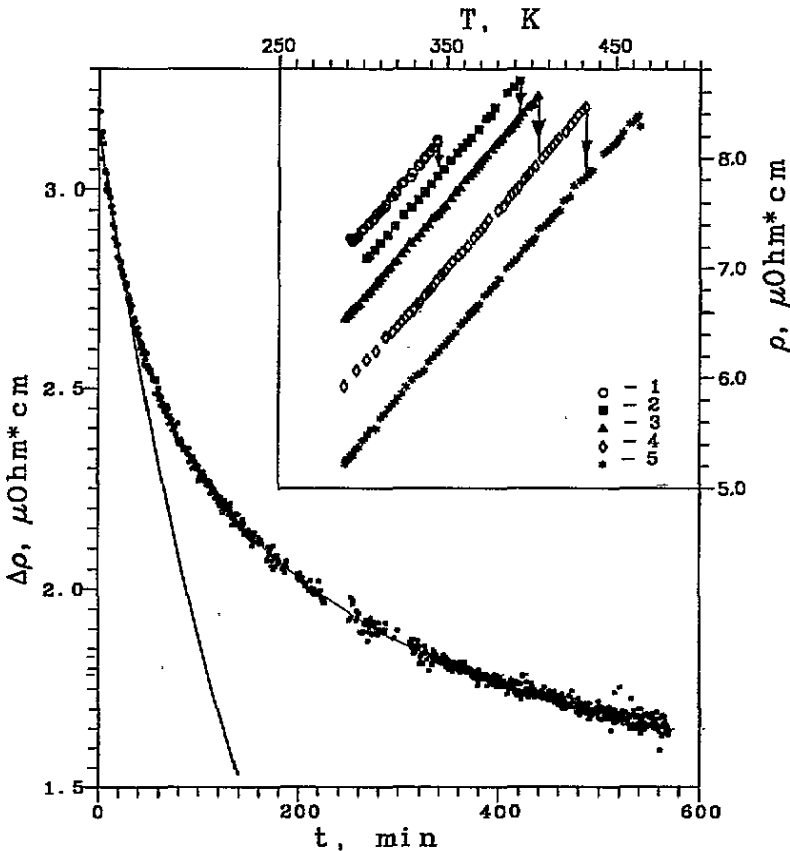


**Figure 1.** An isothermal resistivity relaxation curve  $\Delta\rho(t, T_{\text{an}})$  for  $Al_{0.925}Si_{0.075}$  at  $T_{\text{an}} = 410$  K. In the inset the family of resistivity temperature dependences are shown for  $Al_{0.965}Si_{0.035}$  in the applied 'set of steps' isothermal annealing procedure: 1, starting; 2, after annealing,  $T_{\text{an}} = 380$  K,  $t = 150$  min; 3,  $T_{\text{an}} = 390$  K,  $t = 25$  min; 4,  $T_{\text{an}} = 430$  K,  $t = 10$  min; 5,  $T_{\text{an}} = 450$  K,  $t = 30$  min.

component become dominant. At the same time because of the large segregation tendency the predicted values  $x_{c1}$  and  $x_{c2}$  are not absolutely fine in AlSi and may change slightly with decreasing  $x_c$ . Therefore the appearance of the additional peak in the DSC curves for the Si rich solutions  $x > x_{c2}$  can be connected with the decay of polyatomic Si clusters in the Al based FCC network while the high-temperature peculiarities in  $\dot{H}(T, x_0)$  dependences prevail for the low-concentration limit. It is necessary to point out a correlation between  $\dot{H}(T_{\text{an}})$  and the rate of the isothermal resistivity changes  $d\rho/dt(T_{\text{an}})$  (figure 2). However there is a substantial difference between these two methods, because the DTA and DSC techniques are more sensitive to the changes of metastable phase volume than the resistivity relaxation method. At the same time the latter supplies information on activation energy variation and atomic movement frequencies related to one sample to eliminate differences between samples.

To analyse the resistivity relaxation curves  $\Delta\rho(t, T_{\text{an}}, x_0)$  (figure 1) we applied a transformation to a momentary time scale:

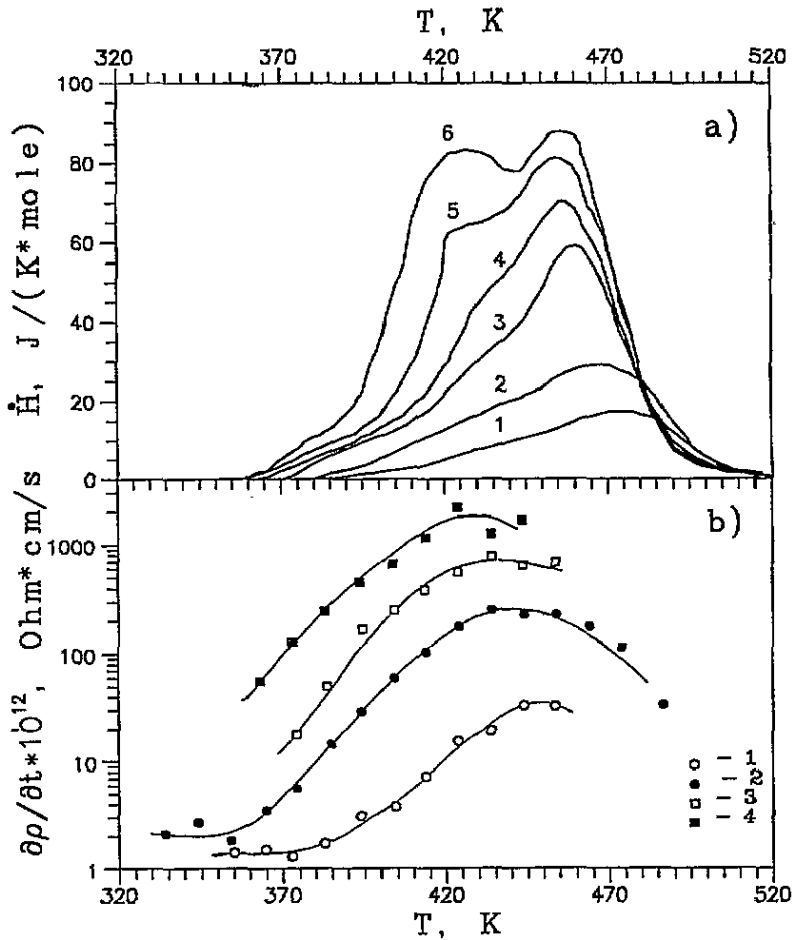


Figure 2. (a) Isochronal DSC curves for  $\text{Al}_{1-x}\text{Si}_x$ : 1,  $x = 0.02$ ; 2,  $x = 0.035$ ; 3,  $x = 0.05$ ; 4,  $x = 0.065$ ; 5,  $x = 0.085$ ; 6,  $x = 0.115$ . (b) Resistivity relaxation rates (see the text) for  $\text{Al}_{1-x}\text{Si}_x$ : 1,  $x = 0.015$ ; 2,  $x = 0.055$ ; 3,  $x = 0.085$ ; 4,  $x = 0.095$ .

$$\tau(t) = -\frac{\Delta\rho(t)}{d(\Delta\rho(t))/dt} \quad (1)$$

(inset in figure 4) and found that the first stage of the decomposition process in  $\text{Al}_{1-x}\text{Si}_x$  corresponds to time independent  $\tau(t)$  behaviour, changing to the  $\tau(t) \sim t$  dependence for the long-time limit. Obviously  $\tau = \text{constant}$  appears after the exponential resistivity relaxation process  $\Delta\rho(t, T_{\text{an}}) \sim \exp(-t/\tau)$  and the linear  $\tau(t)$  behaviour is determined by the relationship  $\Delta\rho \sim t^{-n}$ .

To deduce the exponent  $n$  value the  $\Delta\rho(t, T_{\text{an}})$  dependence was analysed in a double logarithmic scale (figure 4) and the value  $n = 0.22 \pm 0.03$  was obtained. The exponent  $n$  is a good approximation for the resistivity behaviour in the late stage of the relaxation process during time variation over a factor of 10 (figure 4). According to [15] the last stage of the decomposition process with exponent  $n = 0.2$  is in agreement with coagulation of Si polyatomic clusters in the intermediate-temperature region.

Simultaneous  $\Delta\rho(t, T_{\text{an}}, x_0)$  changes appear to be a simple and convenient way to observe the dynamical scaling behaviour in the late stages of the process [16] and the

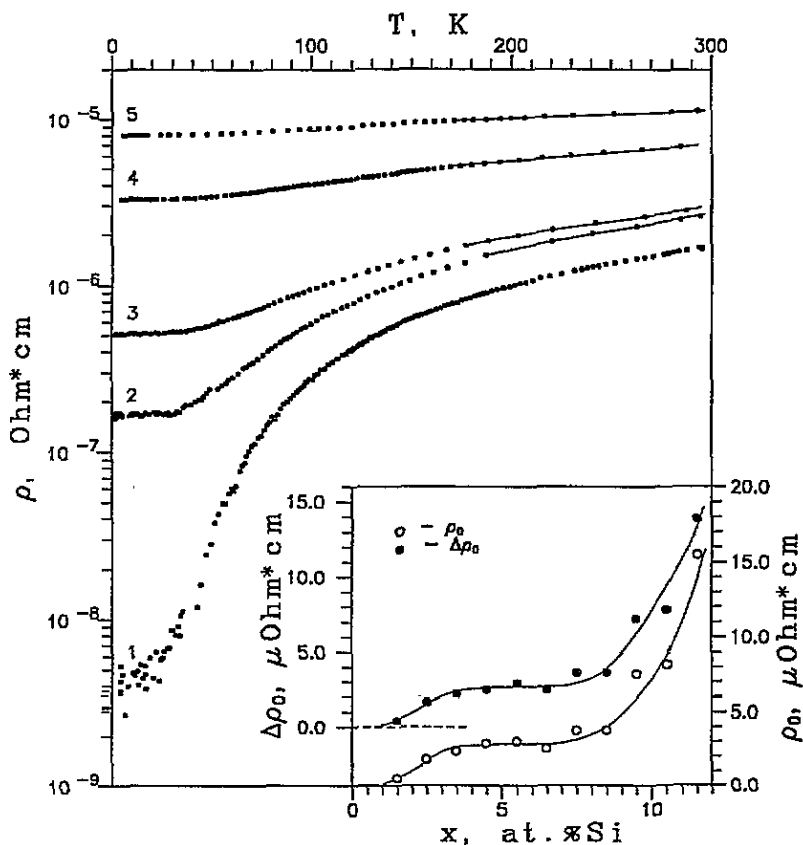


Figure 3. Temperature dependences of resistivity  $\rho(T)$  for Al sample,  $RRR=470$  (1),  $RRR=15$  (2) and solid solutions  $Al_{1-x}Si_x$ ,  $x = 0.015$  (3),  $0.045$  (4),  $0.105$  (5). The inset demonstrates variations of residual resistivity  $\rho_0(T)$  and the metastable part of the resistivity  $\Delta\rho_0(T)$  with the Si concentration in  $Al_{1-x}Si_x$ .

transition from  $n = \frac{1}{5}$  to  $\frac{1}{3}$  is expected when coagulation changes to coalescence [15]. Similar behaviour was established for phase separation in Fe-Cr alloys [17], for example, and the coalescence regime was observed as the last stage for both spinodal decomposition and metastable phase decay [1, 2].

From our data obtained for different Si concentrations  $x$  and annealing temperatures  $T_{an}$  in  $Al_{1-x}Si_x$  we can suppose that up to  $T_{an} = 470$  K and  $t \leq 1000$  min coagulation with  $n \approx 0.2$  dominates as the late stage of the phase transformation process in these alloys.

Then the first process of short-time relaxation (figure 1) was studied precisely by the set of isothermal anneals of  $Al_{1-x}Si_x$  samples (see the inset in figure 1). It should be noted that for any temperature  $T_{an}$  we have recorded only a small part of phase transformation curve to estimate  $d\rho/dt(t \rightarrow 0)$  and  $\rho(\rightarrow 0)$  parameters. A high precision of  $\rho(t, T_{an})$  measurements was achieved by application of a Van der Pauw DC current four-point configuration with an original data processing installation, so the investigated  $Al_{1-x}Si_x$  solid solutions suffered only very slight irreversible changes following the procedure. The family of these 'first-step curves' is shown in the inset of figure 5 and the rates of  $\Delta\rho(t)$  changes are represented in figure 2(b) at different temperatures  $T_{an}$  and Si concentrations  $x$ . One can infer from figure 2(b) that  $d\rho/dt$  increases drastically under variation of temperature

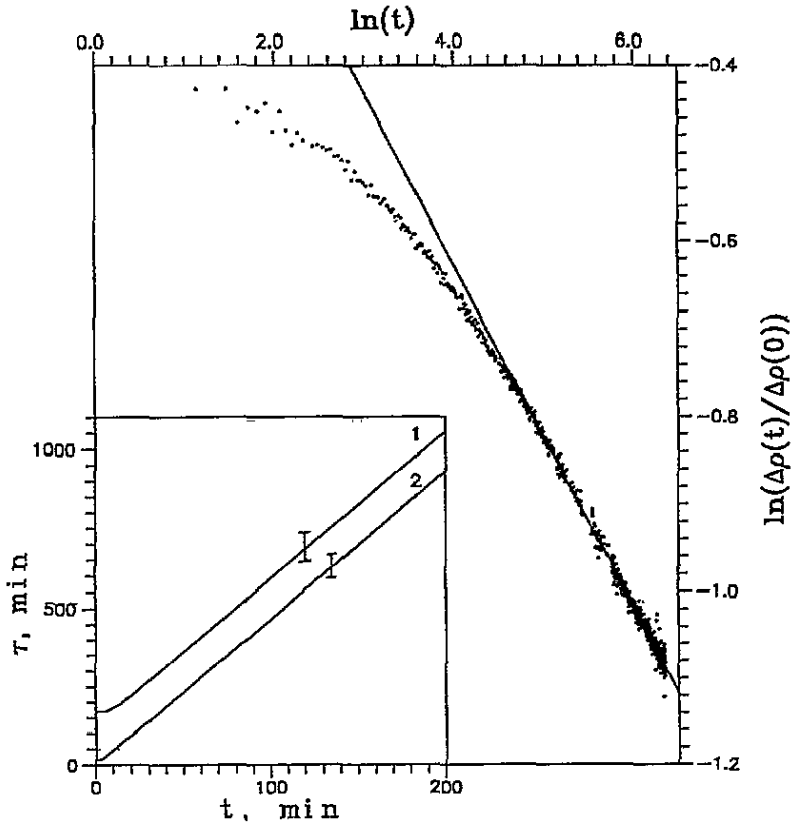


Figure 4. The relaxation curve for  $\text{Al}_{0.925}\text{Si}_{0.075}$  in a logarithmic scale. The momentary time dependences  $\tau(t)$  are shown in the inset for the  $\text{Al}_{0.925}\text{Si}_{0.075}$  sample at different annealing temperatures: 1,  $T_{\text{an}} = 410$  K; 2,  $T_{\text{an}} = 450$  K.

and Si concentration in  $\text{Al}_{1-x}\text{Si}_x$ .

The specification of Arrhenius type coordinates to plot  $\tau(T_{\text{an}})$  dependences in step by step annealing (figure 5) allowed us to estimate the activation law parameters for  $\text{Al}_{1-x}\text{Si}_x$ :

$$\tau = \tau_0 \exp(E_a/k_B T) \quad (2)$$

where  $1/\tau_0$  is the frequency of atomic displacements. From the data of figure 5 one can see also that some preactivated region seems to exist on the low-temperature resistivity relaxation curves  $\Delta\rho(t, T_{\text{an}} \leq 350$  K) for  $x < 0.08$ , which probably appeared after an Si nucleation process in the  $\text{Al}_{1-x}\text{Si}_x$  matrix (see also figure 2(b)) or some kind of slow relaxation of tensions in quenched metals synthesized under high pressure. Using the data of figure 5 and equations (1) and (2) the variation of parameters  $E_a(x)$  and  $\tau_0(x)$  can be obtained in the framework of the proposed procedure. The behaviour of  $E_a(x)$  and  $\tau_0(x)$  appears to be essentially non-monotonic with peculiarities around the value  $x = 0.085$  (figure 6). Simultaneously one can observe that the Arrhenius plotted  $\tau(T_{\text{an}}, x = 0.085)$  curve consists of two different regions that correspond to different values of  $E_a$  and  $\tau_0$ . It should also be mentioned that changes of Si concentration in  $\text{Al}_{1-x}\text{Si}_x$  are followed not only by an increase of activation energy  $E_a$  but also an atomic displacement frequency  $\tau_0^{-1}$  elevation

(figure 6). In the vicinity of the aforementioned concentration  $x \cong 0.085$ , the parameter  $\tau^{-1}(x)$  becomes comparable with phonon frequency values and atomic displacements then determined by thermal motion of atoms in the FCC lattice.

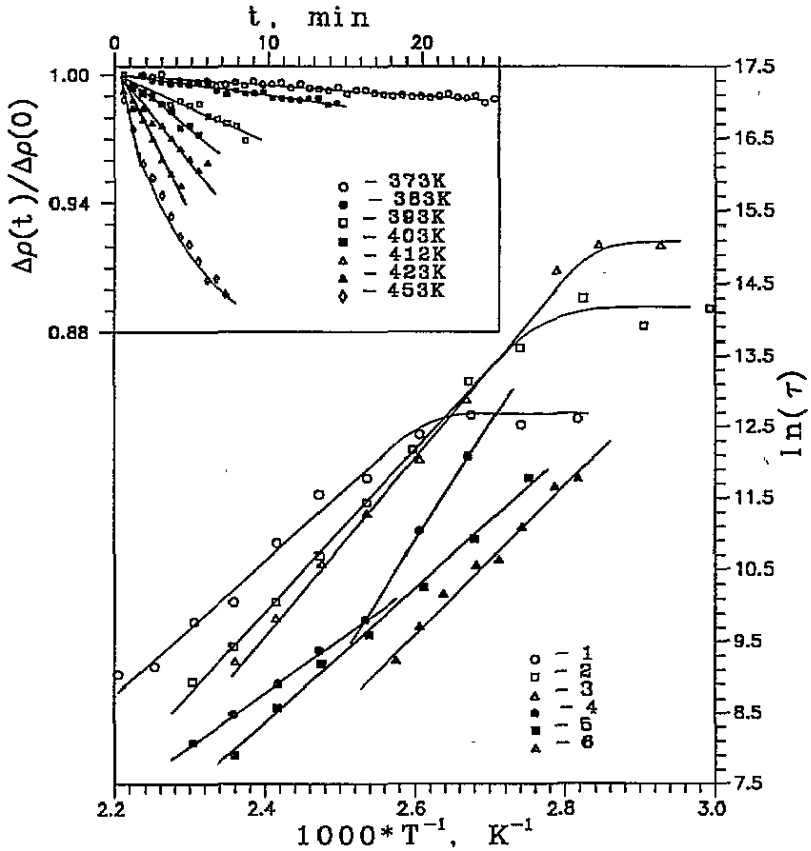


Figure 5. Arrhenius type dependences  $\ln \tau = f(1/T)$  in  $Al_{1-x}Si_x$  solid solutions: 1,  $x = 0.015$ ; 2,  $x = 0.055$ ; 3,  $x = 0.065$ ; 4,  $x = 0.085$ ; 5,  $x = 0.095$ ; 6,  $x = 0.115$ . In the inset the isothermal curves  $\rho(t, T_{an})$  are presented for the sample  $Al_{0.915}Si_{0.085}$  at different annealing temperatures.

These arguments in combination with the superconductive transition temperature  $T_c(x)$  and Hall coefficient  $R_H(x)$  behaviour in supersaturated solid solutions  $Al_{1-x}Si_x$  [18] allow us to suppose that the room temperature spinodal boundary is arranged around  $x = 0.085$  in these non-equilibrium substances.

Then taking into account the dispersion of content  $x$  in solid solution the appearance of two activation sections on the resistivity relaxation curve of  $Al_{0.915}Si_{0.085}$  can be possibly explained by the coexistence of the metastable FCC matrix with  $x \leq 0.085$  and Si rich inclusions produced by the spinodal decomposition process in the sample regions where  $x > 0.085$  values were initially realized. The proposed explanation is successful in explaining also the nature of the decrease of  $E_a$  and  $\tau_0^{-1}$  parameters for  $x \geq 0.09$  (figure 6) and in describing the superconductivity and Hall coefficient anomalies in  $Al_{1-x}Si_x$  [18]. Evidently the same factor is responsible for the appearance of the additional peak of heat



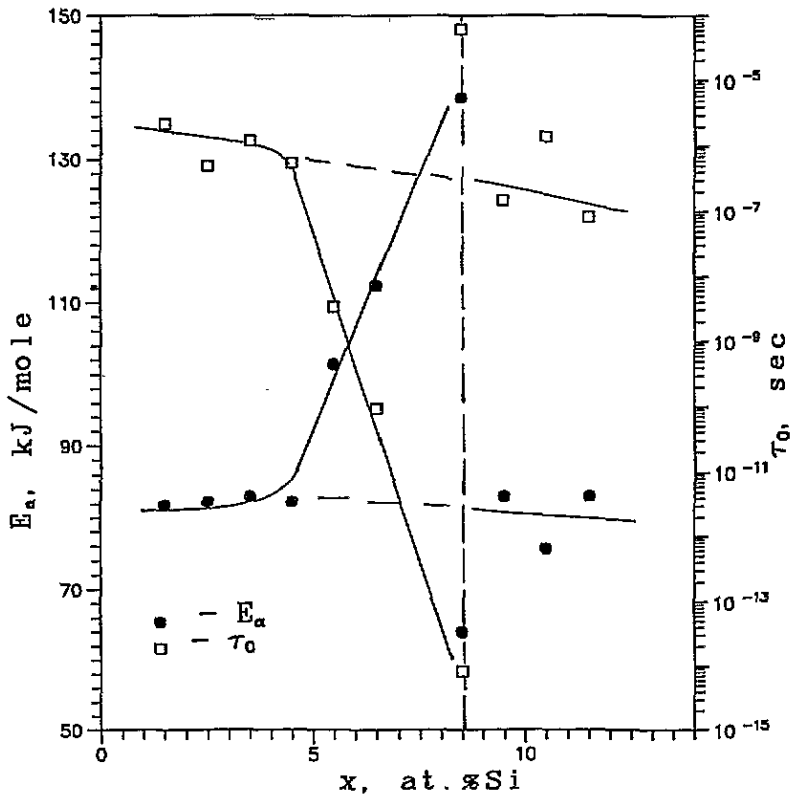


Figure 6. The activation energy  $E_a(x)$  and the  $\tau_0(x)$  coefficient as determined by the resistivity relaxation method for supersaturated  $\text{Al}_{1-x}\text{Si}_x$  solid solutions.

release (figure 2;  $E_{a1} \approx 95 \pm 15 \text{ kJ mol}^{-1} < E_{a2}$ ) which seems to correspond to the polyatomic Si clusters transformation in the FCC matrix of solid solutions.

Moreover the presence of a 'plateau' in the  $\Delta\rho(x)$  and  $\rho_0(x)$  dependences (inset in figure 3) in the interval  $0.035 < x < 0.085$  allows one to suppose that the replacement of Al by Si leads to the appearance of local tensions and the essential distortion of the FCC lattice not only in the vicinity of the Si atom but also around the nearest neighbours of the impurity atom. These significant distortions of bond lengths and angles lead to a broadening of x-ray structure reflexes and even to the appearance of a noticeable diffusion baseline on x-ray scattering intensity curves.

At the same time the structure of Si rich regions that appeared in the  $\text{Al}_{1-x}\text{Si}_x$  samples ( $x \geq 0.085$ ) after spinodal decomposition at room temperature is not visualized absolutely clearly. Indeed x-ray structural analysis data on these samples [9] did not reveal the appearance of a semiconductive Si rich phase in a tetrahedral modification. The problem is closely related to that appearing in [19] for small Si clusters and has been under active discussion for the last few years [20]. Indeed according to results [19] obtained by calculation of the total energy of diamond and FCC fragments as a function of the number of atoms, the metallic structure is favoured over the covalent one for clusters of less than about 50 atoms. Probably in  $\text{Al}_{1-x}\text{Si}_x$  the presence of the FCC lattice causes a more complicated situation. We should mention in this connection the latest results on NMR Al Knight shift  $K(x)$  measurements and Al  $L_{II-III}$  x-ray emission spectra [21] that probably

support the promotion of electron charge density from Al to Si even in the concentration range  $x \leq 0.08$  for  $Al_{1-x}Si_x$ .

Another important feature related to the aforementioned anomaly (figure 6) in the vicinity of the lattice instability limit is an essential increase of Hall mobility at room temperature [21]. The coexistence of these two anomalies in the mobility of electron and atomic subsystems simultaneously with the enhancement of electron-phonon interaction and superconductivity appears to be a very interesting and surprising phenomenon in the behaviour of normal state parameters of non-equilibrium materials.

In conclusion, an intrinsic feature of the supersaturated  $Al_{1-x}Si_x$  solid solutions is their non-equilibrium state and the development of important lattice instability. This lattice instability is caused by the non-equilibrium state of Si in the Al FCC lattice. As a result the measured activation energies are very similar to the  $E_a$  value of Si in the Al matrix [12] and the decomposition process kinetics is determined by thermally activated diffusion of Si atoms in these compounds.

At the same time the situation is very sensitive to Si concentration. For  $x \leq 0.035$  single Si atoms predominate over polyatomic configurations in the FCC matrix and atomic displacements happen with frequency  $10^6$ – $10^7$  Hz. Elevation of  $x$  to 0.085 leads to an increase of activation energy  $E_a$  and atomic displacement frequencies. For  $x \simeq 0.085$ , when Si atoms in the FCC matrix arrange in polyatomic clusters and the  $\tau_0^{-1}$  parameter becomes comparable with phonon frequencies, the spinodal decomposition limit is achieved. The last decay stages of supersaturated  $Al_{1-x}Si_x$  solid solutions are defined as a coagulation process in the wide concentration range  $x \leq 0.1$ . The exponent  $n = 0.2$  was determined for  $T_{an} \leq 470$  K and according to Binder and Stauffer classification [15] identified as a coarsening process that comes about for intermediate temperatures at intermediate times after the complicated initial stage of decomposition.

## Acknowledgments

We would like to thank Professor E G Ponyatovskii and Professor S V Popova for helpful comments. Support for this work was provided by International Science Foundation individual grants for the former Soviet Union scientists.

## References

- [1] Furukawa H 1985 *Adv. Phys.* **34** 703
- [2] Binder K 1991 *Materials Science and Technology* vol 5, ed P Haasen (Weinheim: VCH) ch 7, p 405
- [3] Fratzl P, Yoshida Y, Vogl G and Haubold H J 1992 *Phys. Rev. B* **46** 11 323
- [4] Matyja H, Russell K C, Giessen B C and Grant N J 1975 *Met. Trans. A* **6** 2249
- [5] van Mourik P, Mittermeijer E J and de Keijser Th H 1983 *J. Mater. Sci.* **18** 2706
- [6] Antonione C, Battezzati L and Marino F 1986 *J. Mater. Sci. Lett.* **5** 586
- [7] Mii H, Senoo M and Fujishiro I 1976 *Japan. J. Appl. Phys.* **15** 777
- [8] Banova S M, Korsunskaya I A, Kuznezov G M and Sergeev V A 1978 *Fiz. Met. Met.* **46** 521 (in Russian)
- [9] Degtyareva V F, Chipenko G V, Belash I T, Barkalov O I and Ponyatovskii E G 1985 *Phys. Status Solidi a* **89** K127
- [10] Brazhkin V V, Glushkov V V, Demishev S V, Kosichkin Yu V, Sluchanko N E and Shulgin A I 1993 *J. Phys.: Condens. Matter* **5** 5933
- [11] Khvostancev L G, Vereschagin L F and Novikov A P 1977 *High Temp.-High Pressures* **9** 16
- [12] Chevrier J, Pavuna D and Cyrot-Lackmann F 1987 *Phys. Rev. B* **36** 9115
- [13] Binder K 1986 *Physica A* **140** 35
- [14] Sykes M F and Essam J W 1964 *Phys. Lett.* **133A** 310

- [15] Binder K and Stauffer S 1974 *Phys. Rev. Lett.* **33** 1006  
Binder K 1977 *Phys. Rev. B* **15** 4425
- [16] Binder K and Stauffer S 1976 *Z. Phys. B* **24** 407
- [17] Katano S and Iizumi M 1984 *Phys. Rev. Lett.* **52** 835
- [18] Brazhkin V V, Glushkov V V, Demishev S V, Samarin N A, Sluchanko N E and Shulgin A I to be published
- [19] Chelikowsky J R 1988 *Phys. Rev. Lett.* **60** 2669  
Chelikowsky J R, Glassford K M and Phillips J C 1991 *Phys. Rev. B* **44** 1538
- [20] Jarrold M F and Constant V A 1991 *Phys. Rev. Lett.* **67** 2994  
Kaxiras E and Jackson K 1993 *Phys. Rev. Lett.* **71** 727  
Rothlisberger U, Andreoni W and Parrinello M 1994 *Phys. Rev. Lett.* **72** 665
- [21] Glushkov V V 1993 *Diploma Thesis* Moscow Physics and Technics Institute